Proceeding Paper

Geometric Analysis of LEO-Based Monitoring of GNSS Constellations [†]

Can Oezmaden [1,*], Omar García Crespillo [2], Michael Niestroj [1], Marius Brachvogel [1] and Michael Meurer [1,2]

[1] Chair of Navigation, RWTH Aachen University, 52074 Aachen, Germany; michael.niestroj@nav.rwth-aachen.de (M.N.); marius.brachvogel@nav.rwth-aachen.de (M.B.); michael.meurer@nav.rwth-aachen.de (M.M.)
[2] Institute of Communications and Navigation, German Aerospace Center (DLR), 82234 Wessling, Germany; omar.garciacrespillo@dlr.de
[*] Correspondence: can.oezmaden@nav.rwth-aachen.de; Tel.: +49-241-80900-25
[†] Presented at the European Navigation Conference 2024, Noordwijk, The Netherlands, 22–24 May 2024.

Abstract: The last decade has seen a surge in the development and deployment of low Earth orbit (LEO) constellations primarily serving broadband communication applications. These developments have also influenced the interest providing positioning, navigation, and timing (PNT) services from LEO. Potential services include new ranging signals from LEO, augmentation of global navigation satellite systems (GNSS), and monitoring of GNSS. The latter promises an advantage over existing ground-based monitoring due to the reception of observables with reduced atmospheric error contributions and the potential for lower costs. In this paper, we investigate the influence of LEO constellation design on the line-of-sight visibility conditions for GNSS monitoring. We simulate a series of Walker constellations in LEO with a varying number of total satellites, orbital planes, and orbital heights. From the simulated data, we gather statistics on the number of visible GNSS and LEO satellites, durations of visibility periods, and the quality of this visibility quantified by the dilution of precision (DOP) metric. Our findings indicate that increasing the total number of LEO satellites results in diminishing returns. We find that constellations with relatively few total satellites equally yield an adequate monitoring capability. We also identify orbital geometric constraints resulting in suboptimal performance and discuss optimization strategies.

Keywords: LEO PNT; GNSS monitoring; visibility analysis; constellation design

1. Introduction

Recent breakthroughs in space launch technologies enable the deployment of low Earth orbit (LEO) satellite constellations, which were once deemed to be technologically and financially infeasible. Nowadays, LEO constellations provide earth observation, telecommunications, and broadband internet access services. Lately, public agencies and private companies alike are proposing dedicated LEO constellations to enable new positioning, navigation, and timing (PNT) services [1–3]. Today, PNT services are mainly provided by global navigation satellite systems (GNSS) located in a significantly higher medium Earth orbit (MEO). Besides the widely proposed PNT application, LEO constellations have additionally been suggested for monitoring GNSS medium Earth orbit (MEO) satellites [4]. Due to LEO constellations being above the Earth's atmosphere, GNSS monitoring with low residual atmospheric impact can be performed, giving an advantage over existing ground-based approaches in theory.

A crucial first aspect in designing LEO-based monitoring systems for GNSS is to understand the line-of-sight (LOS) conditions that LEO constellations can provide. Visibility conditions and the expected accuracy via the DOP metrics have been analyzed for various existing and planned LEO constellations [4–7]. However, previous work focused on ground users either by performing monitoring processing from the ground, or by directly using the LEO satellites as ranging sources for PNT. Thus, the visibility conditions between LEO and MEO orbital segments are yet to be further investigated.

Another crucial aspect is the impact a certain constellation design has on the overall performance of a GNSS monitoring system. The constellation optimization literature has been heavily focused on Earth coverage and on providing quality of service to ground users. Walker, multi-Walker, as well as Flower constellation configurations have also been previously studied and optimized at various orbital heights for the DOP metric on the ground [8,9]. Recent LEO-PNT-related studies optimize performance alone [10] or aim to take a holistic approach and optimize cost and performance in conjunction [11]. However, all mentioned strategies either consider one space-based segment and optimize it for the ground, or, when considering two space segments, such as MEO and LEO, still optimize the overall performance for the ground. Thus, an optimal constellation design for observing and monitoring GNSS signals in space from LEO has not been studied.

In this paper, we study the geometric conditions and constraints that can be expected from a LEO-based GNSS monitoring system. We analyze the impact on the overall system performance a certain constellation geometry yields. We conduct simulations on a series of LEO Walker delta constellations at two widely discussed target orbital heights of LEO-PNT systems of 600 km and 1200 km [2,4]. In the course of this, we vary the total number of satellites and the number of orbital planes and investigate the impact of the right ascension of ascending node (RAAN) parameter. During the analysis of our simulated data, we focus on the visibility and observability conditions between the LEO and MEO segments, gathering statistics on figures of merit such as the number of visible satellites, the duration of visibility, and the DOP values for each time instant.

2. Methodology

2.1. Geometrical Analysis

2.1.1. Availability

For quantifying the availability metric of the investigated LEO-based monitoring service, we first define the following two terms. We refer to *visibility* when evaluating MEO GNSS satellites visible to any single LEO satellite. And we contrast it to *observability* when we refer to the capacity at which any single and same MEO GNSS satellite is observed by the designed LEO constellation.

In the case of visibility of MEO satellites to LEO satellites, we can apply an intuitive visibility criterion by considering an elevation mask. This is accomplished by first converting the local Cartesian coordinates into spherical coordinates consisting of azimuth, elevation, and range. Thus, for any time instance t, we can define a set of visible MEO satellites to the i-th LEO satellite as

$$\mathcal{M}_{i,\,\mathrm{vis}}(t) = \{m \in \mathcal{M}\,|\,\theta_{i,m}(t) \geq \theta_{\mathrm{mask}}\}, \tag{1}$$

where $\mathcal{M}$ refers to the set of all MEO satellites, m to a specific MEO satellite, and $\theta_{i,m}(t)$ represents the elevation of the m-th MEO satellite as seen by the i-th LEO satellite in the Earth ellipsoid-referenced local East North Up-frame (ENU) of the LEO satellite. In this frame, we assume the GNSS antenna of the LEO satellite points in the positive Up direction

away from the surface of the Earth. The size of this set represents the number of visible MEO satellites to the i-th LEO satellite, so that

$$|\mathcal{M}_{i,\text{vis}}(t)| = M_{i,\text{vis}}(t). \tag{2}$$

Conversely, for the observability, we consider a set of LEO satellites $\mathcal{L}_{m,\text{obs}}(k)$, obtaining observations of the m-th MEO satellite for the observation time instant k. This set can be defined by considering the occurrences of the m-th MEO satellite being visible across all LEO satellites $\mathcal{L}$. The number of this occurrence is equal to $L_{m,\text{obs}}(k)$, so that

$$|\mathcal{L}_{m,\text{obs}}(k)| = L_{m,\text{obs}}(k). \tag{3}$$

Physically, this means that the observables of the m-th MEO satellite are to be collected from $L_{m,\text{obs}}(k)$ LEO satellites. It also stems from the elevation mask visibility criterion introduced in Equation (1).

2.1.2. Dilution of Precision (DOP)

The next metric we evaluate is the potential accuracy of the monitoring service stemming solely from the geometry of the utilized satellite constellations. An important metric for this consideration is the concept of DOP. When computed in a local-horizontal coordinate frame, the DOP can be projected into the position domain and quantify how a given visibility geometry affects the measurement error variance. As such, it is an important figure of merit in GNSS-related constellation design. Using the set of visible MEO satellites, we can define the geometry matrices for GPS and Galileo separately for the i-th LEO satellite at any time instant as

$$\boldsymbol{H}_{i,\text{G}} = \left[\left[\boldsymbol{u}_i^{(1)} \cdots \boldsymbol{u}_i^{(M_{\text{vis, G}})} \right]^{\text{T}} \quad \mathbb{1}_4^{\text{T}} \right] \quad \text{and} \quad \boldsymbol{H}_{i,\text{E}} = \left[\left[\boldsymbol{u}_i^{(1)} \cdots \boldsymbol{u}_i^{(M_{\text{vis, E}})} \right]^{\text{T}} \quad \mathbb{1}_4^{\text{T}} \right] \tag{4}$$

where $\boldsymbol{H}_{i,\text{G}}$ and $\boldsymbol{H}_{i,\text{E}}$ denote the geometry matrix of GPS and Galileo, respectively, as seen from the i-th LEO satellite, $\boldsymbol{u}_i^{(m)}$ denotes a unit line-of-sight (LOS) vector pointing from the i-th LEO satellite to the m-th MEO satellite defined in the Earth ellipsoid-referenced ENU coordinate frame, and $\mathbb{1}_4$ denotes a vector of ones of length 4. To evaluate the DOP, we perform the following mathematical transformations on the geometry matrices:

$$\text{GDOP} = \sqrt{\text{tr}\left(\left(\boldsymbol{H}^{\text{T}} \boldsymbol{H} \right)^{-1} \right)}, \tag{5}$$

where GDOP denotes the geometric DOP across three spatial and single time dimensions. Similarly, we can define a three-dimensional spatial positional DOP (PDOP) metric, which measures the level of observability of MEO satellites from

$$\boldsymbol{H}_{m,\text{G}} = \left[\boldsymbol{u}_m^{(1)} \cdots \boldsymbol{u}_m^{(L_{\text{G, obs}})} \right]^{\text{T}} \quad \text{and} \quad \boldsymbol{H}_{m,\text{E}} = \left[\boldsymbol{u}_m^{(1)} \cdots \boldsymbol{u}_m^{(L_{\text{E, obs}})} \right]^{\text{T}}. \tag{6}$$

2.2. Simulation Environment

In this paper, we developed a simulator named LEONAS (LEO Navigation System Simulator), which acts as a wrapper around the MATLAB Satellite Communications Toolbox and Stanford's MAAST [12] and defines its own set of utility functions. A scenario object is defined using the MATLAB Satellite Communications Toolbox provided with a set of parameters. Satellite constellations are loaded into the scenario by parsing the YUMA almanac files from the configuration. LEO constellations are defined as Walker delta constellations and their almanac is saved by LEONAS in the YUMA format. Figure 1

visualizes a selection of LEO constellations studied in this paper, whereas Table 1 lists all relevant simulation configuration parameters and their used value.
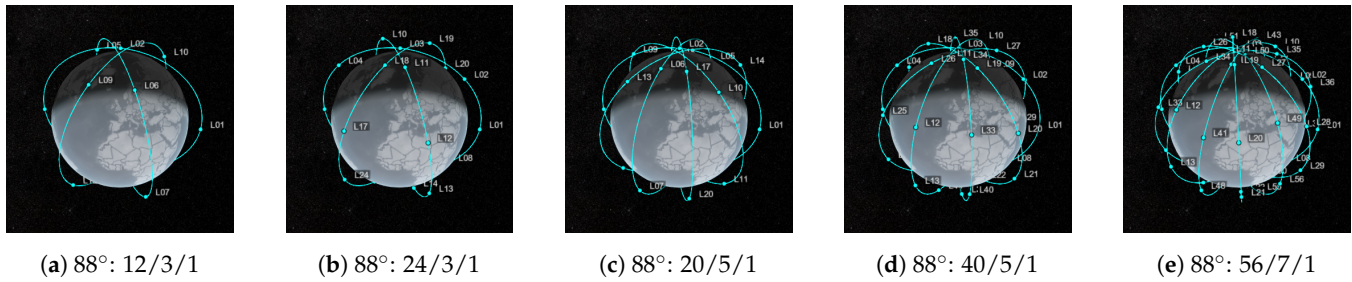

(**a**) 88°: 12/3/1   (**b**) 88°: 24/3/1   (**c**) 88°: 20/5/1   (**d**) 88°: 40/5/1   (**e**) 88°: 56/7/1

Figure 1. A selection of LEO Walker delta constellations simulated in this paper. Walker notation: $i : t/p/f$, where i denotes inclination, t is the total number of satellites, p is the number of orbital planes, and f is the phasing factor.

Table 1. Table of simulation parameters and their values used for the results unless specified otherwise.

Parameter	Used Value
Initial time t_{start}	2024-02-18 00:00 UTC
End time t_{end}	2024-03-19 00:00 UTC
Simulation rate δt_{s}	60 s
Orbit propagator	Two-body Keplerian
Satellite Constellations	GPS, Galileo, and LEO
GPS Almanac File	MAAST almgps24+3.txt
Galileo Almanac File	MAAST almgalileo.txt

The results of the orbit propagation are written to disk and saved in MATLAB's MAT-File format version 7.3. This allows compatibility with HDF, a widely accepted data encapsulation format in the scientific community. A log file containing a list of events of the simulator is saved alongside the results. The log file contains a header including metadata such as the version of LEONAS that produced the results, thus enabling the reproducibility of the research data.

3. Results

3.1. Visibility

We begin to examine the results of our simulations by considering a LEO satellite looking up away from the surface of the Earth towards the MEO GNSS satellites. In Figure 2, we visualize the worst-case visibility LEO satellite in an 88°: 24/3/1 Walker delta constellation situated 1200 km above the Earth, evaluated for an elevation mask of $\theta_{\text{mask}} = 5°$. This allows us to gain insight into the dynamics of the system. As such, we find the worst-case satellite experiences a minimum of 5 visible GPS satellites at around 9:00 UTC. This can be directly correlated to the experienced and sustained worsening of the GPS GDOP at the same time. It is worth noting, however, that the worst constellation geometry appears to happen at approx. 16:00 UTC. For this instance, we correlate the dip of the visible satellite number to 5. In general, we found Galileo satellites to be visible in greater numbers and with better geometry according to lower GDOP values.

We can add more context to the performance of the whole constellation by examining the statistical distribution of these temporal quantities over a longer simulation duration. This is presented in Figure 3 by gathering simulated data over a month. We observed the minimum number of visible satellites remaining at 5 for GPS. We also observed across the whole LEO constellation that Galileo satellites are more frequently visible compared to GPS. This is evident from the histogram in Figure 3a, and by the general color difference of the heatmaps in Figure 3d,e. The median values for visible GPS and Galileo satellites

are 8 and 10, respectively. We also observed Galileo visibility durations to be shorter than those of GPS. This is most evident from the so-called survivor function based on the empirical cumulative distribution function (ECDF) in Figure 3c. The dashed 95%-th percentile confidence line is crossed at around 1000 s for Galileo and at around 1500 s for GPS. This quantity is to be interpreted as 95% of all visibility durations that are longer than 1000 s and 1500 s. The reason for shorter visibility durations may be linked to a greater orbital velocity difference between LEO and Galileo, compared to LEO and GPS.
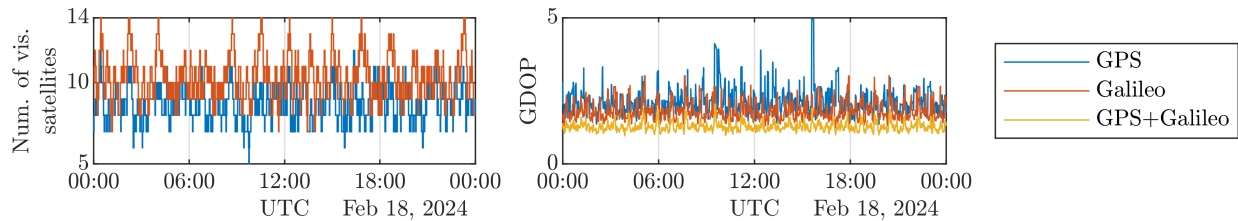

Figure 2. Time series of number of visible GNSS satellites and GDOP values for a single LEO in a 1200 km 88°: 24/3/1 constellation.
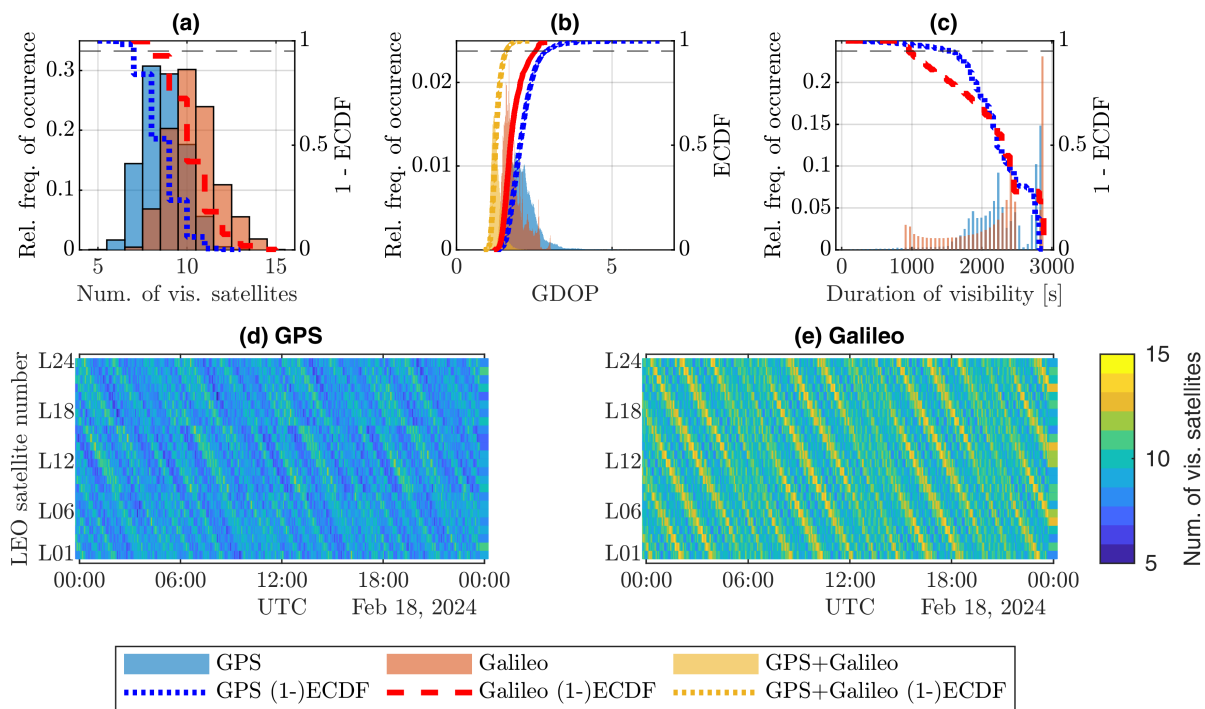

Figure 3. Histograms of number of visible GNSS satellites (**a**), their GDOP (**b**), duration of visibilities (**c**), and heatmaps over time of Global Positioning System (GPS) (**d**) and Galileo (**e**) visibility for the LEO constellation 1200 km 88°: 24/3/1, $\Omega = 0°$. Horizontal thin dashed dark line represents the 95% confidence mark. Data simulated for a duration of a month, time series visualized for a day. Visibility evaluated for $\theta_{mask} = 5°$.

3.2. Observability

We repeated the same analysis in the other direction by considering a single MEO satellite looking down in its nadir direction and by analyzing LEO satellites providing observables for this MEO satellite. Figure 4 presents the results of this for the same 1200 km 88°: 24/3/1 constellation. As seen in Figure 4, we found the number of LEO satellites observing particular MEO satellites G01 and E01 to oscillate periodically between 4 and 10. This oscillation is not surprising, as it is linked to the highly regular Walker Delta constellation utilized for the LEO segment.
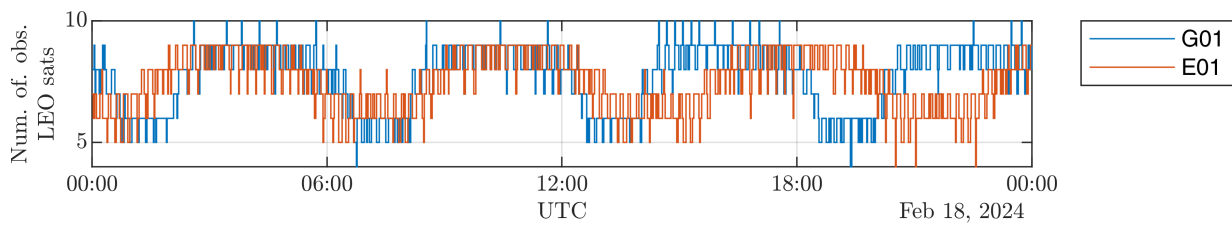
Figure 4. Time series of number of observing LEO satellites for GPS G01 and Galileo E01 using a LEO Walker delta constellation 1200 km 88°: 24/3/1, $\Omega = 0°$.

In Figure 5, we visualize the statistics gathered from all MEO satellites being observed by the configured LEO constellation. In Figure 5a, we found the number of observing LEO satellites for both constellations to be greater than 5 for 95% of the time. In Figure 5b, we found the three-dimensional PDOP to be around 3-4 for both GPS and Galileo. The higher average values of PDOP in comparison to visibility GDOP in Figure 3b are expected, since the distribution of LEO satellites seen down from a MEO satellite is a lot more compact in comparison to the other direction. Geometrically, this is due to the ratio between the surface area of a smaller LEO sphere and a larger MEO sphere.
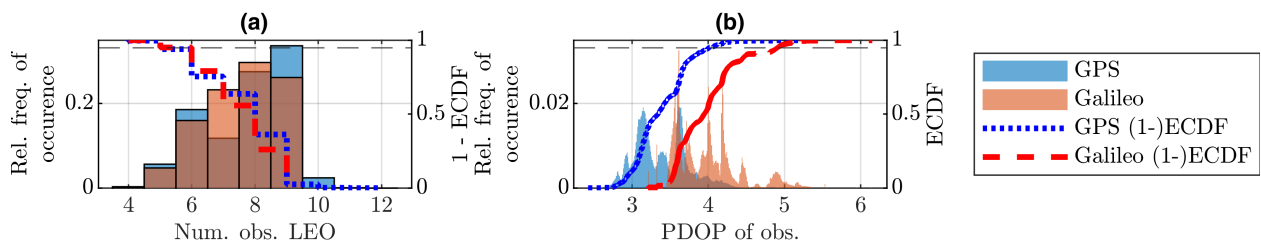

Figure 5. Distribution of the number of observing LEO satellites for GPS and Galileo (**a**), and the corresponding distribution of PDOP values (**b**). Horizontal thin dashed dark line represents the 95% confidence mark.

3.3. Overview

To provide an overview of the simulated constellation configuration, we present the results compared across three configurations in Table 2. The configurations selected here are Walker delta 36/3/1, 35/5/1, and 35/7/1, all at 88° inclination, 1200 km orbital height, and at $\Omega = 0°$. The reason for the selection of these configurations is to isolate the effect that the number of orbital planes has on the performance of monitoring. Due to their innate geometry, Walker delta constellations only allow an odd number of orbital planes. We chose to investigate LEO constellations with three, five, and seven LEO orbital planes with a minimum of four satellites per plane. The closest and smallest common divisor for three, five, and seven orbital planes is 36 and 35. This analysis allows for a meaningful comparison of the effect of the number of planes parameter. A more extensive comparison of the results across all simulation configurations can be found in Tables 3 and 4. For both orbital heights, constellations with a low number of total satellites, such as 12/3/1, have merely two LEO satellites providing observables for the same MEO satellite at a given time, making the 3D spatial monitoring impossible. This is again reflected in the maximum PDOP from 12/3/1 being infinitely large. Overall, visibility conditions tend to stay the same, whereas the observability gets better with the increasing number of total satellites, as expected.

Table 2. Comparison of geometrical analysis for LEO constellation configurations with roughly the same amount of satellites distributed across a varying number of orbital planes. Values calculated with an elevation mask $\theta_{\text{mask}} = 5°$. The numbers are provided in the order of $P_{0.95}$ (min, med, max).

	36/3/1		35/5/1		35/7/1	
Num. vis. GPS	7	(5, 9, 13)	7	(4, 9, 13)	7	(4, 9, 13)
Num. vis. GAL	8	(7, 10, 15)	7	(6, 10, 15)	7	(6, 10, 15)
Vis. dur. GPS [min]	26	(1, 37, 48)	22	(1, 37, 49)	22	(1, 37, 48)
Vis. dur. GAL [min]	16	(1, 39, 48)	22	(1, 35, 48)	24	(1, 39, 48)
GDOP GPS	2.9	(1.3, 2.0, 6.6)	2.9	(1.2, 2.0, 47)	2.9	(1.2, 2.0, 51)
GDOP GAL	2.5	(1.2, 1.7, 3.0)	2.6	(1.2, 1.8, 3.3)	2.6	(1.2, 1.8, 3.3)
GDOP GPS+GAL	1.6	(0.9, 1.3, 2.4)	1.6	(0.9, 1.3, 2.7)	1.6	(0.9, 1.3, 2.6)
Num. LEO obs. GPS	8	(7, 12, 15)	8	(6, 12, 15)	8	(5, 12, 15)
Num. LEO obs. GAL	9	(8, 12, 15)	8	(6, 11, 15)	8	(5, 11, 14)
Obs. PDOP GPS	3.2	(2.1, 2.7, 3.8)	3.3	(2.1, 2.7, 4.1)	3.2	(2.2, 2.8, 12)
Obs. PDOP GAL	3.6	(2.6, 3.2, 3.9)	3.8	(2.6, 3.2, 4.7)	3.7	(2.6, 3.3, 14)

Table 3. Overview of all metrics for $h_{\text{LEO}} = 600\,\text{km}$. Value order: $P_{0.95}$ (min, med, max). Durations accurate up to simulation rate ($\pm 60\,\text{s}$).

	12/3/1		24/3/1		20/5/1		40/5/1		28/7/1		56/7/1	
Num. vis. GPS	7	(5, 9, 13)	7	(5, 9, 13)	7	(5, 9, 13)	7	(4, 9, 13)	7	(5, 9, 13)	7	(5, 9, 13)
Num. vis. GAL	9	(7, 11, 15)	9	(7, 11, 15)	8	(6, 10, 15)	8	(6, 10, 15)	8	(6, 10, 15)	8	(6, 10, 15)
Vis. dur. GPS [min]	24	(1, 34, 42)	24	(1, 34, 42)	21	(1, 34, 42)	21	(1, 34, 43)	21	(1, 34, 43)	21	(1, 34, 43)
Vis. dur. GAL [min]	17	(1, 35, 43)	17	(1, 35, 43)	21	(1, 35, 43)	21	(1, 36, 43)	22	(1, 36, 43)	22	(1, 36, 43)
GDOP GPS	2.8	(1.2, 2.0, 6.0)	2.8	(1.2, 2.0, 6.2)	2.8	(1.2, 2.0, 8.5)	2.8	(1.2, 2.0, 18)	2.8	(1.2, 2.0, 14)	2.8	(1.2, 2.0, 14)
GDOP GAL	2.5	(1.2, 1.7, 3.1)	2.5	(1.2, 1.7, 3.1)	2.6	(1.2, 1.8, 3.4)	2.6	(1.2, 1.8, 3.4)	2.6	(1.2, 1.8, 3.4)	2.6	(1.2, 1.8, 3.4)
GDOP GPS+GAL	1.5	(0.9, 1.2, 2.3)	1.5	(0.9, 1.2, 2.4)	1.6	(0.9, 1.3, 2.6)	1.6	(0.9, 1.3, 2.5)	1.6	(0.9, 1.2, 2.5)	1.6	(0.9, 1.2, 2.6)
Num. LEO obs. GPS	2	(2, 4, 6)	6	(4, 8, 12)	4	(3, 7, 10)	10	(8, 14, 20)	6	(4, 10, 14)	14	(10, 19, 25)
Num. LEO obs. GAL	3	(2, 4, 6)	6	(5, 8, 10)	4	(3, 6, 10)	9	(8, 13, 16)	6	(5, 9, 13)	13	(11, 19, 23)
Obs. PDOP GPS	9.8	(3.6, 5.9, ∞)	1.3	(0.9, 1.1, 1.7)	2.3	(1.0, 1.3, ∞)	1.0	(0.7, 0.9, 1.2)	1.8	(0.9, 1.1, 4.6)	0.8	(0.6, 0.7, 1.1)
Obs. PDOP GAL	11	(4.3, 7.3, ∞)	1.3	(1.0, 1.2, 1.5)	2.6	(1.0, 1.4, ∞)	1.0	(0.8, 0.9, 1.1)	2.0	(0.9, 1.1, 4.0)	0.8	(0.7, 0.7, 0.9)

Table 4. Overview of all metrics for $h_{\text{LEO}} = 1200\,\text{km}$. Value order: $P_{0.95}$ (min, med, max). Durations accurate up to simulation rate ($\pm 60\,\text{s}$).

	12/3/1		24/3/1		20/5/1		40/5/1		28/7/1		56/7/1	
Num. vis. GPS	7	(4, 9, 13)	7	(5, 9, 13)	7	(4, 9, 13)	7	(4, 9, 13)	7	(4, 9, 13)	7	(4, 9, 13)
Num. vis. GAL	8	(7, 10, 15)	8	(7, 10, 15)	7	(6, 10, 15)	7	(6, 10, 15)	7	(6, 10, 15)	7	(6, 10, 15)
Vis. dur. GPS [min]	26	(1, 37, 48)	26	(1, 37, 48)	22	(1, 37, 49)	22	(1, 37, 49)	23	(1, 37, 48)	22	(1, 37, 48)
Vis. dur. GAL [min]	16	(1, 39, 48)	16	(1, 39, 48)	22	(1, 39, 48)	22	(1, 39, 48)	24	(1, 39, 48)	24	(1, 39, 48)
GDOP GPS	2.7	(1.2, 2.0, 5.9)	2.8	(1.2, 2.0, 6.2)	2.8	(1.2, 2.0, 8.5)	2.8	(1.2, 2.0, 17)	2.8	(1.2, 2.0, 14)	2.8	(1.2, 2.0, 14)
GDOP GAL	2.7	(1.2, 1.7, 3.1)	2.5	(1.2, 1.7, 3.1)	2.6	(1.2, 1.8, 3.3)	2.6	(1.2, 1.8, 3.4)	2.6	(1.2, 1.8, 3.4)	2.6	(1.2, 1.8, 3.4)
GDOP GPS+GAL	1.5	(0.9, 1.2, 2.3)	1.5	(0.9, 1.2, 2.4)	1.5	(0.9, 1.3, 2.6)	1.5	(0.9, 1.3, 2.5)	1.6	(0.9, 1.2, 2.5)	1.6	(0.9, 1.2, 2.6)
Num. LEO obs. GPS	2	(2, 4, 6)	5	(4, 8, 12)	4	(3, 7, 10)	9	(6, 13, 19)	6	(4, 9, 14)	13	(10, 19, 25)
Num. LEO obs. GAL	2	(2, 4, 6)	6	(4, 8, 9)	4	(3, 6, 10)	9	(6, 13, 15)	6	(4, 9, 13)	13	(11, 18, 21)
Obs. PDOP GPS	3.4	(1.3, 2.6, ∞)	4.0	(2.4, 3.3, 5.5)	2.4	(1.0, 1.3, ∞)	1.0	(0.7, 0.9, 1.3)	1.9	(0.9, 1.1, 4.6)	0.8	(0.6, 0.7, 1.1)
Obs. PDOP GAL	4.0	(1.4, 2.5, ∞)	4.9	(3.2, 3.9, 6.2)	2.7	(1.1, 1.4, ∞)	1.0	(0.8, 0.9, 1.3)	2.1	(0.9, 1.1, 4.6)	0.8	(0.7, 0.7, 1.0)

4. Discussion

During our investigation, we noticed anomalies in the calculated DOP value for GPS. This is especially true for configurations with a high number of orbital planes (e.g., maximum GPS GDOP of 51 from the 35/7/1 constellation in Table 2). We claim these events are fundamentally caused by the geometry mismatch between the utilized Walker LEO constellations and the irregular distribution of GPS satellites across their nominal six orbital planes. We further investigated the temporal and spatial distribution of such events causing the poor performance across a set of Fibonnaci-distributed points [13] evenly distributed on the surface of a sphere at both design altitudes $h_{\text{LEO}} = 600\,\text{km}, 1200\,\text{km}$. The simulation duration for this analysis was chosen to be 12 h to capture a whole GPS orbital period. The results of this investigation are presented in Figures 6 and 7, where the

Fibonnaci-distributed points are projected onto a 2D map, representing the inertial latitude and longitudes.
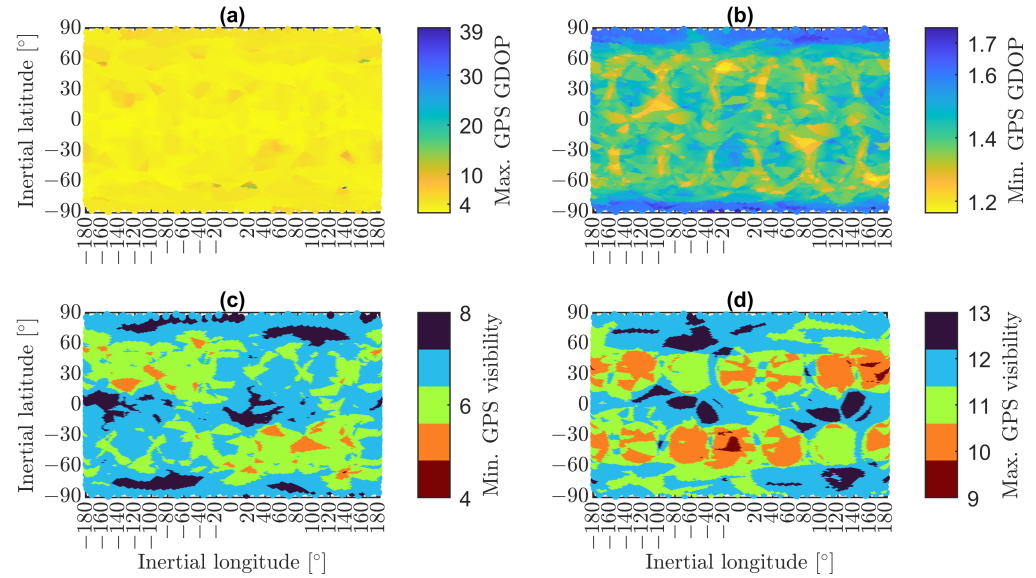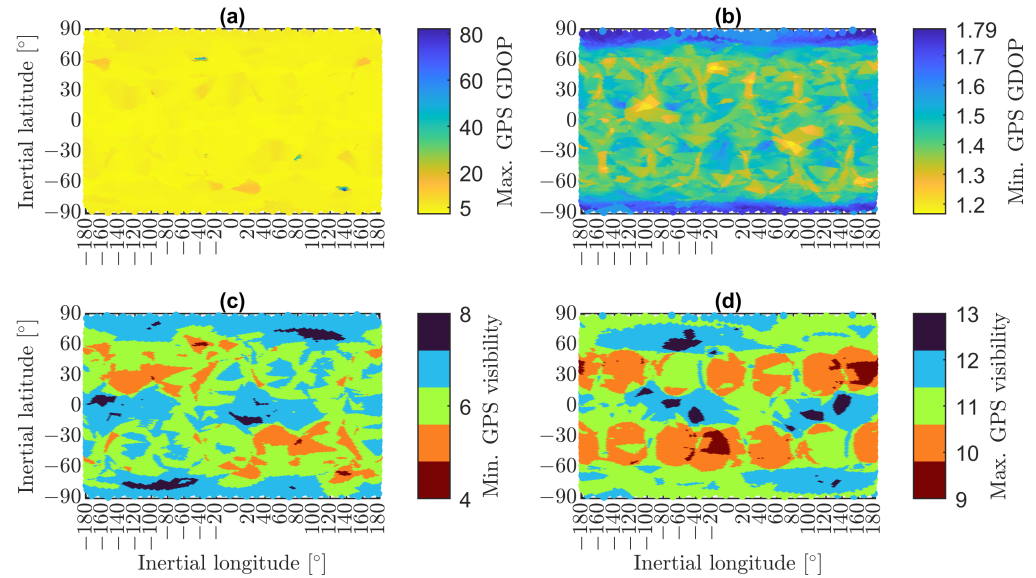

Figure 6. Number of visible GPS satellites in the worst case (**c**) and the best case (**d**) scenarios, and corresponding DOP values in the worst case (**a**) and the best case scenarios (**b**) as seen from a grid of points on a sphere located at $h_{\text{LEO}} = 600\,\text{km}$. Evaluated for an elevation mask $\theta_{\text{mask}} = 5°$.

Figure 7. Number of visible GPS satellites in the worst case (**c**) and the best case (**d**) scenarios, and corresponding DOP values in the worst case (**a**) and the best case scenarios (**b**) as seen from a grid of points on a sphere located at $h_{\text{LEO}} = 1200\,\text{km}$. Evaluated for an elevation mask $\theta_{\text{mask}} = 5°$.

Figures 6a and 7a visualize the worst case DOP, whereas Figures 6b and 7b visualize the best case DOP. It is worth noting that the GDOP value is higher on average for the 1200 km orbit. In both cases, a region of high GDOP values is observed at a latitude of around $-70°$ and at $140°$ of inertial longitude. In this region, there is a possibility of the number of visible GPS satellites plummeting to four, as evident in Figures 6c and 7c. For the 1200 km LEO orbit, a GDOP value of as high as 80 was obtained, as seen in Figure 7a. The higher 1200 km LEO constellation also has even larger areas with high DOP values, such as the region with 20 DOP stretching from $0°$ to $35°$ longitude at approx $-70°$ latitude.

We argue that one can carefully design a LEO constellation around these high-DOP regions of GPS. Due to their known spatial distributions, the RAAN parameter of the constellation can be varied in order to place orbital planes avoiding the high-DOP regions. This gets harder with the increasing number of orbital planes due to the limited space available for shifting.

5. Conclusions

In this paper, we lay important groundwork for the performance analysis of LEO-based GNSS monitoring systems. We have carried out our investigations solely based on the geometries of the constellations. As such, we aimed to remain agnostic of any system parameters such as signals, satellite hardware, and accompanying ground segments, to widen the applicability of our findings. Our findings highlight several guidelines in designing a successful LEO constellation for GNSS monitoring purposes. The total number of satellites does not need to exceed 24, which also has beneficial cost implications for the whole system. With 24 satellites in three orbital planes, an adequate visibility with a minimum of five visible MEO satellites and the observability of a single MEO satellite with at least four LEO satellites was found. Increasing the number of orbital planes, while keeping the same number of satellites, is found to be counterproductive in two ways. Firstly, it results in worsened observability of MEO satellites due to the reduction in the number of satellites per orbital plane. Secondly, it increases the launch and constellation maintenance costs. During our survey of LEO constellation configurations, we found regions of extremely high GPS DOP values at both design altitudes of 600 km and 1200 km. These high GPS DOP regions occur statically in the inertial spatial dimension of the constellation, and possess a high dynamic range temporally. A low number of orbital planes again has been found to provide an advantage, since there is more headroom in avoiding these regions on the sphere in comparison to more dense LEO constellations.

Author Contributions: Conceptualization, C.O., O.G.C. and M.M.; methodology, C.O.; software, C.O.; validation, C.O., O.G.C., M.N., M.B. and M.M; formal analysis, C.O.; investigation, C.O.; resources, C.O.; data curation, C.O.; writing—original draft preparation, C.O.; writing—review and editing, O.G.C. and M.M.; visualization, C.O.; supervision, O.G.C. and M.M; project administration, O.G.C.; funding acquisition, M.M. All authors have read and agreed to the published version of the manuscript.

Institutional Review Board Statement: Not applicable.

Informed Consent Statement: Not applicable.

Data Availability Statement: The raw data supporting the conclusions of this article will be made available by the authors upon request.

Conflicts of Interest: The authors declare no conflicts of interest.

References

1. Reid, T.G.; Chan, B.; Goel, A.; Gunning, K.; Manning, B.; Martin, J.; Neish, A.; Perkins, A.; Tarantino, P. Satellite Navigation for the Age of Autonomy. In Proceedings of the 2020 IEEE/ION Position, Location and Navigation Symposium (PLANS), Portland, OR, USA, 20–23 April 2020; pp. 342–352. [CrossRef]
2. González, A.; Tobías; Rodriguez, I.; Navarro, P.; Sobrero, F.; Carbonell, E.; Calle, D.; Fernández, J. LEO Satellites for PNT, the Next Step for Precise Positioning Applications. In Proceedings of the 35th International Technical Meeting of the Satellite Division of The Institute of Navigation (ION GNSS+ 2022), Denver, CO, USA, 19–23 September 2022; pp. 2573–2581. [CrossRef]

3. Ries, L.; Limon, M.C.; Grec, F.C.; Anghileri, M.; Prieto-Cerdeira, R.; Abel, F.; Miguez, J.; Perello-Gisbert, J.V.; D'addio, S.; Ioannidis, R.; et al. LEO-PNT for Augmenting Europe's Space-based PNT Capabilities. In Proceedings of the 2023 IEEE/ION Position, Location and Navigation Symposium (PLANS), Monterey, CA, USA, 24–27 April 2023.

4. Catalán, C.C.; Iglesias, L.G.; Muñoz, A.J.; Matamala, E.F.; Berges, C.P.; Moreno, A.M.; Gassió, M.P.; Fort, E.A.; Samper, M.D.L.; Álvarez, J.B.; et al. Integrity Monitoring of GNSS with LEO Satellites to Reduce the Time to Alarm. In Proceedings of the 36th International Technical Meeting of the Satellite Division of the Institute of Navigation (ION GNSS+ 2023), Denver, CO, USA, 11–15 September 2023; pp. 2282–2309.

5. Morales-Ferre, R.; Lohan, E.S.; Falco, G.; Falletti, E. GDOP-based Analysis of Suitability of LEO Constellations for Future Satellite-Based Positioning. In Proceedings of the 2020 Annual IEEE International Conference on Wireless for Space and Extreme Environments (WiSEE), Vicenza, Italy, 12–14 October 2020; pp. 147–152.

6. Ge, H.; Li, B.; Jia, S.; Nie, L.; Wu, T.; Yang, Z.; Shang, J.; Zheng, Y.; Ge, M. LEO Enhanced Global Navigation Satellite System (LeGNSS): Progress, Opportunities, and Challenges. *Geo-Spat. Inf. Sci.* **2022**, *25*, 1–13. [CrossRef]

7. Ferre, R.M.; Lohan, E.S. Comparison of MEO, LEO, and Terrestrial IoT Configurations in Terms of GDOP and Achievable Positioning Accuracies. *IEEE J. Radio Freq. Identif.* **2021**, *5*, 287–299. [CrossRef]

8. Dufour, F.; Bertrand, R.; Sarda, J.; Lasserre, E.; Bernussou, J. Constellation Design Optimization with a DOP Based Criterion. In Proceedings of the 14th International Symposium on Space Flight Dynamics, Foz do Iguaçu, Brazil, 8–12 February 1999.

9. Casanova, D.; Avendaño, M.; Mortari, D. Seeking GDOP-optimal Flower Constellations for Global Coverage Problems through Evolutionary Algorithms. *Aerosp. Sci. Technol.* **2014**, *39*, 331–337. [CrossRef]

10. Ge, H.; Li, B.; Nie, L.; Ge, M.; Schuh, H. LEO Constellation Optimization for LEO Enhanced Global Navigation Satellite System (LeGNSS). *Adv. Space Res.* **2020**, *66*, 520–532. [CrossRef]

11. Marchionne, L.; Gessato, L.M.; Toni, F.; Barbera, S.L. Striking a Balance: Performance and Cost Optimization of LEO-PNT Constellation for Hybrid Users Using a Meta-Heuristic Approach. In Proceedings of the 2023 IEEE 10th International Workshop on Metrology for AeroSpace, MetroAeroSpace 2023—Proceedings, Milan, Italy, 19–21 June 2023; pp. 609–614. [CrossRef]

12. Jan, S.S.; Chan, W.; Walter, T. MATLAB Algorithm Availability Simulation Tool. *GPS Solut.* **2009**, *13*, 327–332. [CrossRef]

13. González, Á. Measurement of Areas on a Sphere Using Fibonacci and Latitude–Longitude Lattices. *Math. Geosci.* **2010**, *42*, 49–64. [CrossRef]